CELL CYCLE
2021, VOL. 20, NO. 18, 1875–1889
https://doi.org/10.1080/15384101.2021.1963910

Taylor & Francis
Taylor & Francis Group

RESEARCH PAPER

P76RBE silencing inhibits ovarian cancer cell proliferation, migration, and invasion via suppressing the integrin β1/NF-κB pathway

Limei Yan, Zeping He, Wei Li, Ning Liu, and Song Gao

Department of Obstetrics and Gynecology, Shengjing Hospital of China Medical University, Shenyang, Liaoning, China

ABSTRACT

Rhophilin Rho GTPase binding protein 2 (P76RBE) belongs to rhophilin family of Rho-GTPase-binding proteins and is found to contribute to the development of diverse cancers. Data in Oncomine and Kaplan–Meier Plotter databases showed that P76RBE was upregulated in ovarian cancer tissues compared with normal tissues, and patients with high P76RBE expression had worse overall survival, which indicated P76RBE may be associated with the pathogenesis of ovarian cancer. This study aimed to investigate the role of P76RBE in ovarian cancer and to reveal the possible underlying mechanisms. The results demonstrated that P76RBE was highly expressed in ovarian cancer tissues and ovarian cancer cell lines. Functionally, silencing of P76RBE suppressed the proliferation, induced cell cycle arrest, and inhibited migration and invasion in OVCAR-3 and OV-90 cells, while overexpression of P76RBE showed opposite effects on A2780 cells. Mechanically, P76RBE silencing resulted in downregulation of integrin β1, accompanying the reduced NF-κB p65 phosphorylation and nuclear translocation. Importantly, integrin β1 knockdown effectively rescued the effects of P76RBE overexpression on ovarian cancer cells with suppressed proliferation, migration, and invasion. Additionally, in the xenograft tumors derived from OVCAR-3 and OV-90 cell lines, P76RBE knockdown inhibited tumor growth. Meanwhile, the expression of integrin β1 and NF-κB p65 phosphorylation was decreased. In summary, our findings indicate that P76RBE contributes to the progression of ovarian cancer through regulating the integrin β1/NF-κB signaling, and it may be a promising target for ovarian cancer therapy.

ARTICLE HISTORY
Received 21 April 2021
Revised 26 July 2021
Accepted 29 July 2021

KEYWORDS
P76RBE; ovarian cancer; integrin β1/NF-κB pathway

1. Introduction

Ovarian cancer is one of the most common malignant tumors with the poor prognosis. It has become the deadliest threat to women. Data from epidemiology show that the 5-year survival rate of patients is less than 45% [1]. Although the application of chemotherapy and radiotherapy has greatly improved the treatment, patients with recurrent ovarian cancer are still incurable [2]. Moreover, most patients are diagnosed with advanced stage due to no early symptoms, which also prevents effective treatment [3]. Consequently, it is meaningful to discover genes with differential expression and determine their mechanisms participated in the ovarian cancer initiation and metastasis processes.

Rhophilin Rho GTPase binding protein 2 (P76RBE) located on chromosome 9q13.11 takes part in organization of the actin cytoskeleton [4]. Related studies have demonstrated that P76RBE is associated with various types of cancers, including prostate cancer, malignant glioma, and non-small cell lung cancer (NSCLC) [5–7]. In addition, rs10411210, the genetic variant of P76RBE, is also considered as a prognostic biomarker for patients with colorectal cancer [8]. Thus, we suspect that P76RBE might also play an important role in ovarian cancer. Additionally, it has been documented that P76RBE triggers RhoA activation in malignant glioma. RhoA activation is involved in a series of biological processes such as cell proliferation and metastasis [9,10]. Knockdown of RhoA suppresses these malignant behaviors in ovarian cancer [11]. Interestingly, we observe that integrin β1, a regulatory factor of RhoA, is overexpressed in ovarian cancer cells [12,13]. Studies show that the activation of integrin β1 mediates the formation of malignant phenotype of ovarian cancer cells [14,15]. However, the relationship

CONTACT Song Gao gaosong_sj@163.com

between P76RBE and integrin β1 in ovarian cancer cells remains unclear.

Transcription factors as a nuclear genetic determinant of tumorigenesis usually become potential targets for anti-tumor drugs [16]. Nuclear transcription factor kappa B (NF-κB), one of the crucial transcription factors, acts as a master regulator of cell proliferation and invasion. NF-κB is involved in many diseases including cancer [17]. Furthermore, it is reported that integrin β1 intermediates NF-κB signaling promoting tumor development [18]. Nevertheless, little is known regarding the connection between P76RBE and NF-κB. In the current study, we intended to investigate the effect of P76RBE on ovarian cancer *in vitro* and *in vivo*.

2. Materials and methods

2.1. Cell culture

The human ovarian cancer cell lines OV-90, SK-OV-3, OVCAR-3, A2780, and normal ovarian epithelial cells were purchased from Procell Life Science & Technology Co., Ltd (Wuhan, China). The OV-90, OVCAR-3, and normal ovarian epithelial cells were cultured in their own special medium obtained from Procell (CM-0626, CM-0178, CM-H055). The SK-OV-3 cells were grown in McCoy's 5A medium with 10% fetal bovine serum (FBS; 11,011–8611, Tianhang, Zhejiang, China). The A2780 cells were incubated in DMEM medium (12,100–46, Gibco, Thermo Fisher Scientific, USA) contained 10% FBS. All cell lines were maintained at 37°C containing 5% CO_2.

2.2. Lentivirus vector construction and cell transduction

Lentiviral expressing P76RBE shRNA (Lv-shRNA1-P76RBE and Lv-shRNA2-P76RBE) and the negative control, Lv-shRNA-NC, were obtained from Sangon Biotech, Shanghai, China. OVCAR-3 and OV-90 cells were infected with lentivirus particles for 72 h followed by flow sorter constructing stable infected cells.

In addition, the P76RBE overexpression vector (Ov-P76RBE) and control vector (Vector) were purchased from GenScript, Nanjing, China. Integrin β1 small interfering RNA (siRNA) and siNC were purchased from JTS scientific, Wuhan, China. The integrin β1 siRNA sequences were as follows: sense, 5′-GGAGGAUUACUUCGGACUUTT-3′, anti-sense, 5′-AAGUCCGAAGUAAUCCUCCTT-3′. A2780 cells were transfected with Ov-P76RBE/Vector/Integrin β1 siRNA/siNC using Lipofectamine 3000 (L3000015, Invitrogen, USA) for 48 h. The collected cells were used for following experiments.

2.3. Western blot analysis

Total protein was extracted using RIPA lysate (R0010, Solarbio, Beijing, China) plus phenylmethanesulfonyl fluoride (PMSF; P0100, Solarbio), and the concentration of which was further quantified by BCA kit (PC0020, Solarbio). The samples were separated via sodium dodecyl sulfate-polyacrylamide gel electrophoresis (SDS-PAGE; D1010, Solarbio) following transferred to polyvinylidene fluoride (PVDF; IPVH00010, Millipore, USA) membranes. Subsequently, membranes were blocked with skim milk (A600669, Sangon Biotech, Shanghai, China), washed via tris buffered saline with tween-20 (TBST), and incubated with specific primary antibodies for overnight at 4°C. The primary antibodies were listed as follows: anti-integrin β1 (1:500 dilution, 12,594-1-AP, Proteintech, Wuhan, China), anti-cyclin E1 (1:1000 dilution, A14225, Abclonal, Wuhan, China), anti-P76RBE (1:1000 dilution, 12,671-1-AP, Proteintech), anti-PCNA (1:1000 dilution, A12427, Abclonal), anti-MMP2 (1:500 dilution, 10,373-2-AP, Proteintech), anti-MMP9 (1:1000 dilution, 10,375-2-AP, Proteintech), anti-p-P65 (1:500 dilution, AP0475, Abclonal), anti-P65 (1:1000 dilution, AF5006, Affinity, Jiangsu, China), anti-IκBα (1:500 dilution, A19714, Abclonal), anti-COX2 (1:1000 dilution, A1253, Abclonal), anti-GAPDH (1:1000 dilution, 60,004-1-Ig, Proteintech). After being washed with TBST for four times, membranes were incubated with the goat-anti-rabbit secondary antibody (1:3000 dilution, SE134, Solarbio) at 37°C for 1 h. The signals were monitored via enhanced chemiluminescence (ECL; PE0010,

Solarbio). The bands were obtained followed by analyzing the gray value.

2.4. Immunofluorescence

The cells were fixed with 4% paraformaldehyde for 15 min followed by covering 0.1% tritonX-100 at room temperature for 30 min. After washing with phosphate buffer saline (PBS), the cells were added onto goat serum about 15 min. The cells were incubated with anti-P76RBE (1:50 dilution, Proteintech) and anti-P65 (1:200 dilution, Affinity) at 4°C overnight. Then, the cells were washed with PBS and incubated with Cy3-labeled goat-anti-rabbit secondary antibody (1:200 dilution, A0516, Beyotime, Jiangsu, China) for 60 min in the darkness. Following dropping the 4′,6-diamidino-2-phenylindole (DAPI, D106471, Aladdin, Shanghai, China) to counterstain the nucleus, the fluorescence pictures were captured with a fluorescence microscope.

2.5. MTT assay

Cell viability was evaluated using MTT assay. In brief, cells (4×10^3 cells/well) were seeded in 96-well plates. Cells were incubated with the complete medium containing MTT (0.5 mg/ml, KGA311, KeyGen Biotech, Nanjing, China) at 0 h, 24 h, 48 h, 72 h, and 96 h, respectively. After incubation for 4 h, the supernatant was removed, and DMSO (150 µl/well, ST038, Beyotime) was added to dissolve the formazan. Ten minutes later, the OD values were detected via microplate reader (BIOTEK, USA) at 570 nm.

2.6. Colony formation

A total of 300 cells were grown in a petri dish with a diameter of 60 mm. Approximately 2 weeks, the obvious colonies formed. PBS was used to wash cells and paraformaldehyde (4%) was added for fixing 25 min. Cells were stained with Wright's-Giemsa assay reagent (KGA227, KeyGen Biotech) for 5 min. Following, the image was captured, and the number of colonies was counted.

2.7. Flow cytometry analysis

Flow cytometry (Aceabio, USA) was applied to analyze cell cycle distribution by cell cycle kit (C1052, Beyotime). Briefly, the cells were harvested followed by centrifugation in 1000 *g* for 5 min. After pre-cooling with 70% ethanol, cells were fixed at 4°C for 2 h. The ethanol was discarded via centrifugation, and cells were washed using PBS. Following resuspension in 500 µl staining buffer, propidium iodide (PI, 25 µl), and RNase A (10 µl) were added to cells for incubation 30 min at 37°C in the dark according to cell cycle kit's instruction (C1052, Beyotime). The cell cycle distribution was analyzed by flow cytometry (Aceabio, USA).

2.8. Transwell assay

Matrigel Invasion Assay: The Matrigel (356,234, BD, USA) was thawed at 4°C overnight, and then was diluted with serum-free medium. The transwell chamber (3422, Corning, USA) was placed into 24-well plates before the diluted Matrigel was covered. When the Matrigel was solidified, 200 µl cell suspension (2×10^4 cells/well) was added in the apical chamber and 800 µl complete medium included 10% FBS was given in the basolateral chamber. Cells were incubated in the incubator (condition: 37°C and 5% CO_2) for 24 h prior to 4% paraformaldehyde fixation. Whereafter, cells were stained with crystal violet (0528, Amresco, USA) for about 3 min. The number of cells that had invaded the lower side of the chamber was counted using a microscope.

Migration assay: In brief, 200 µl cell suspension (6×10^3 cells/well) were added in the upper chamber, and the lower chamber contained 800 µl complete medium. Following incubation for 24 h, cells were stained with crystal violet. Subsequently, images of cells migrating into the lower chamber were captured.

2.9. Gelatin zymography

The effect of P76RBE on MMP2 and MMP9 activities was monitored via gelatin zymography. The cell supernatant was collected and separated from SDS-PAGE with 70 V for 2.5 h. Following, the gel

was eluted and rinsed for 40 min and 20 min, respectively. The gel was incubated with incubation solution for 40 h at 37°C prior to Coomassie brilliant blue (0472, Amresco, USA) staining. The gelatinolytic bands were obtained via imaging instrument, and the intensity was analyzed.

2.10. Xenografts in nude mouse

The nude mice aged 6–8 weeks were freely feed 1 week for adaption. The experiments were approved by the Committee of Shengjing Hospital of China Medical University. Subsequently, nude mice were subcutaneously injected with OV90 or OVCAR3 cells infected with Lv-shRNA-NC, Lv-shRNA1-P76RBE, and Lv-shRNA2-P76RBE, respectively. When the tumor was formed, the tumor volume was measured every 3 days. Mice were sacrificed via intraperitoneal injection sodium pentobarbital (50 mg/kg) on the 22th day. The images of tumor tissues were captured.

2.11. Immunohistochemistry

After dehydration and permeabilization, the tumor tissues were embedded into paraffin and cut into 5 μm sections. The sections were dewaxed using xylene, ethanol, distilled water, and PBS, respectively. After antigen retrieval, the sections were incubated with hydrogen peroxide. The sections were blocked with goat serum, and then incubated with primary antibodies for 24 h overnight (anti-P76RBE, 1:50 dilution; anti-integrin β1, 1:50 dilution). The sections were labeled with the HRP-goat-anti-rabbit secondary antibody (#31,460, Thermo Fisher Scientific) prior to DAB (DA1010, Solarbio) and hematoxylin staining. Following dehydrating with a gradient ethanol system, the expression of P76RBE and integrin β1 was observed under a microscope with 400 × .

2.12. Data analysis

All data were displayed with mean ± standard deviation and analyzed via GraphPad Prism 8.0. The one-way analysis of variance (ANOVA) was applied to compare the differences among multiple groups followed by *Bonferroni's test*. A value of $p < 0.05$ was regarded significant.

3. Results

3.1. P76RBE expression is increased in ovarian cancer tissues and cell lines

Data obtained from Oncomine database showed that P76RBE was overexpressed in the ovarian cancer tissues compared with that of normal tissues (Figure 1(a)). Kaplan–Meier Plotter database analysis illustrated that ovarian cancer patients with high P76RBE expression had worse overall survival compared to that of patients with low P76RBE expression (Figure 1(b)). In addition, results of real-time PCR demonstrated that P76RBE expression was increased in the ovarian cancer tissues compared to that in the normal ovarian tissues (Figure 1(c)). Furthermore, we also determined the expression of P76RBE in the human ovarian cancer cell lines and normal ovarian epithelial cells via western blot (Figure 1(d)) and immunofluorescence (Figure 1(e)). The results showed that compared with the normal cells, P76RBE was also upregulated in OV-90, SK-OV-3, OVCAR-3, and A2780 cells.

3.2. P76RBE knockdown suppresses ovarian cancer cell proliferation in vitro

To explore the functions of P76RBE in ovarian cancer, OVCAR-3, and OV-90 cells with the higher P76RBE expression were selected for the following experiments. We established P76RBE-knockdown cell lines via lentiviral expressing P76RBE shRNA, and the downregulated P76RBE protein expression confirmed the infection efficiency (Figure 2(a)). Following, cell growth curves received from MTT assays were used to exhibit the effect of P76RBE silencing on cell viability at different time points, which indicated that cell viability was inhibited after P76RBE knockdown at 24 h, 48 h, 72 h, and 96 h (Figure 2(b)), $p < 0.01$). Moreover, the colony formation experiments also demonstrated that silencing of P76RBE decreased the number of colonies in OVCAR-3 ($P < 0.01$) and OV-90 cells ($P < 0.001$) (Figure 2(c)). Besides, flow cytometry was carried out to examine the cell cycle distribution, which exhibited that silencing of P76RBE arrested ovarian cancer cells at G1 phase (Figure 3(a)), $p < 0.05$). Furthermore, the expression levels of cell cycle-related proteins were assessed via western blot

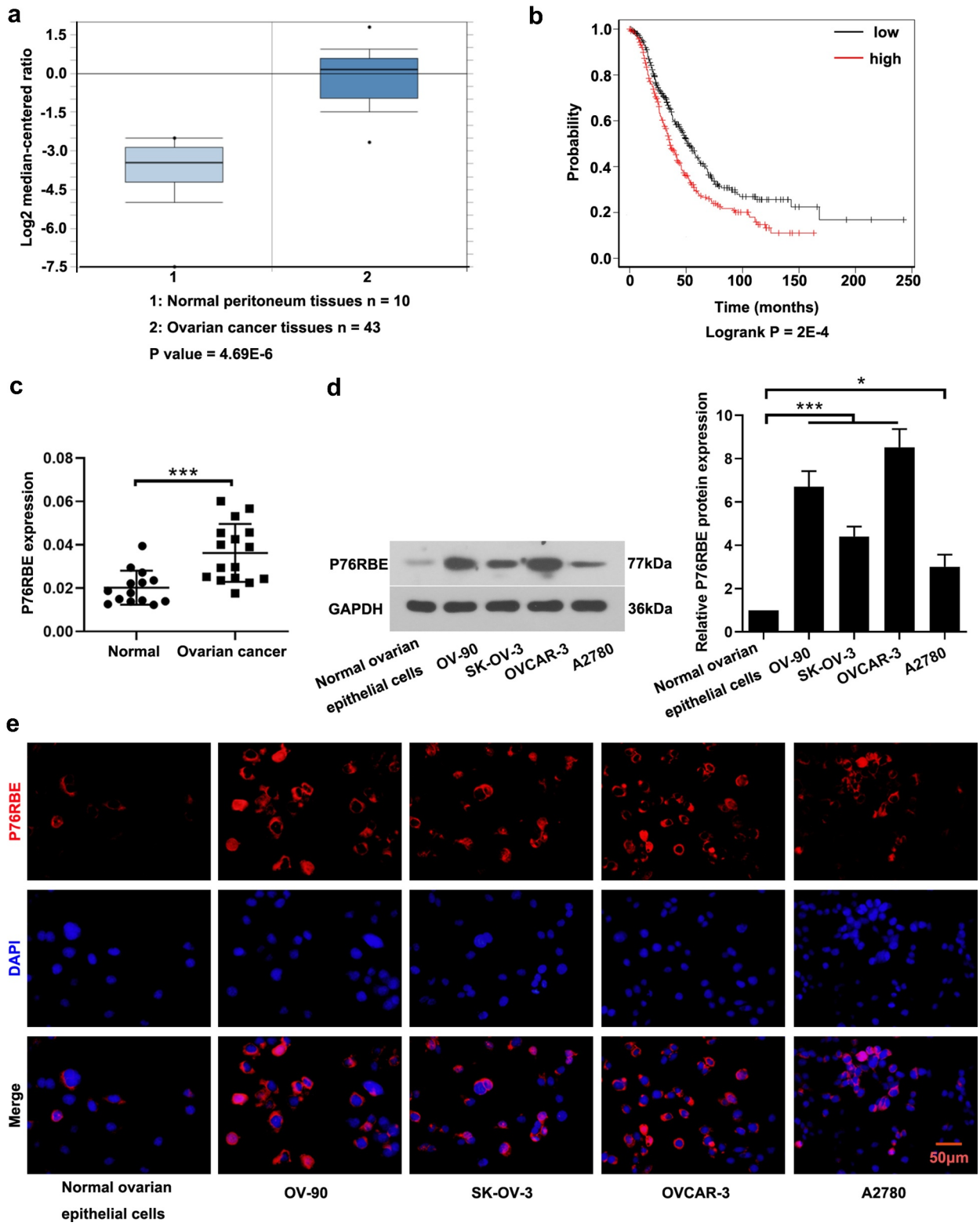

Figure 1. P76RBE is overexpressed in ovarian cancer. (a) The P76RBE expression in normal peritoneum tissues (n = 10) and ovarian cancer tissues (n = 43). (b) Kaplan–Meier Plotter database showed overall survival in ovarian cancer patients with high and low P76RBE expression. (c) Real-time PCR detected the P76RBE expression in normal ovarian tissues (n = 14) and ovarian cancer tissues (n = 16). Western blot (d) and immunofluorescence (e) were applied to detect the expression levels in the human ovarian cancer cell lines OV-90, SK-OV-3, OVCAR-3, A2780, and normal ovarian epithelial cells, respectively. (scale bar = 50 μm). *P < 0.05 and ***P < 0.001.

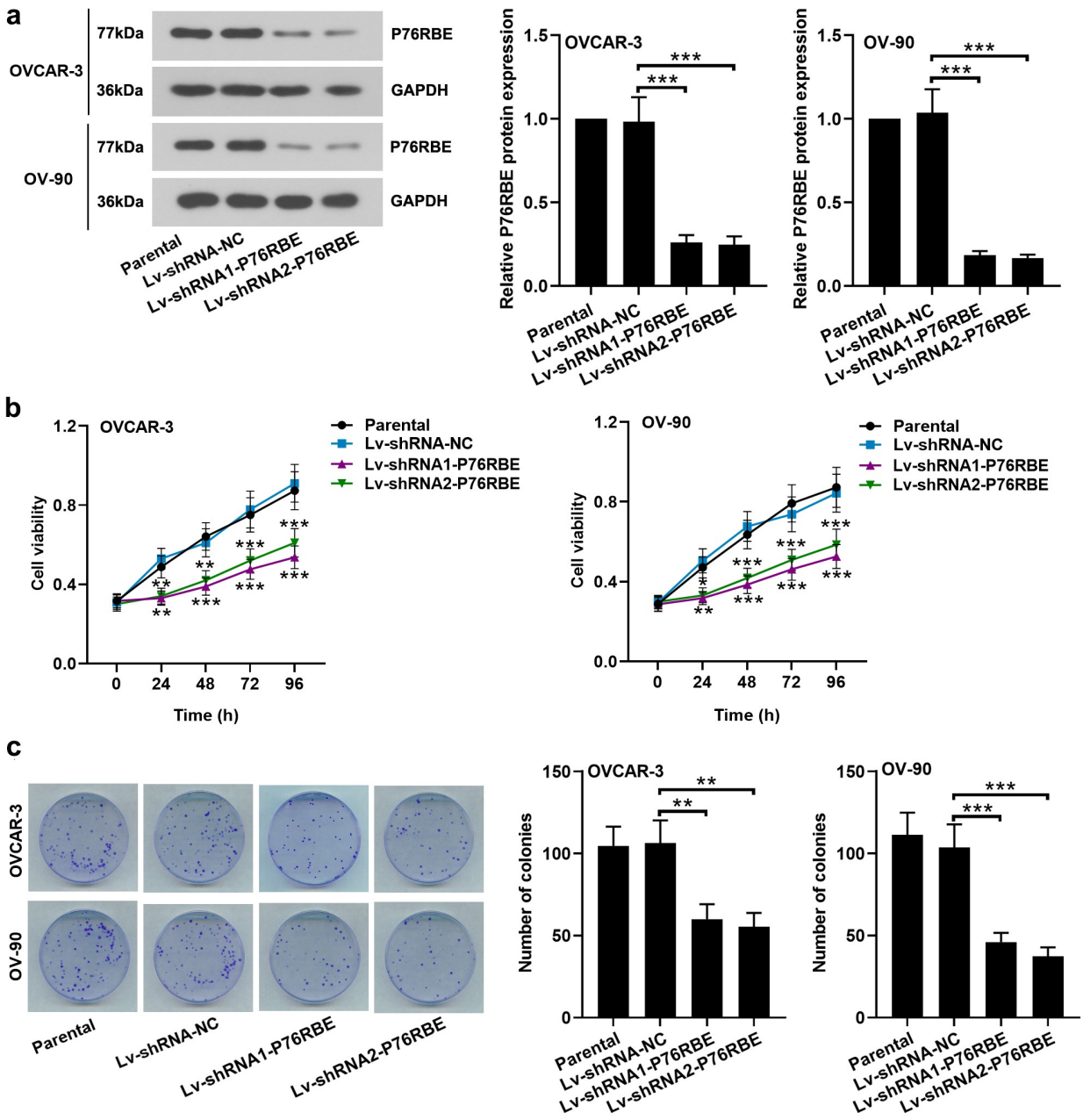

Figure 2. P76RBE knockdown suppresses ovarian cancer cell growth *in vitro*. (a) The protein expression of P76RBE in OVCAR-3 and OV-90 infected with Lv-shRNA1-P76RBE, Lv-shRNA2-P76RBE, or Lv-shRNA-NC, were evaluated via western blot. (b) Cell growth curves were used to exhibit the effect of silencing P76RBE on cell viability at different time points (0 h, 24 h, 48 h, 72 h, and 96 h). (c) Colony formation assay was carried out to assess cell proliferation, whilst the number of colonies was calculated. * represents *vs*. Lv-shRNA-NC. *P < 0.05, **P < 0.01, ***P < 0.001.

analysis. Both PCNA and cyclin E1 expressions were diminished in P76RBE-siliencing cells than those of control (Figure 3(b)). All data suggested that P76RBE promoted ovarian cancer cell proliferation.

3.3. *P76RBE silencing attenuates ovarian cancer cell migration and invasion* in vitro

Further, the transwell chambers with or without Matrigel were executed to estimate the effect of

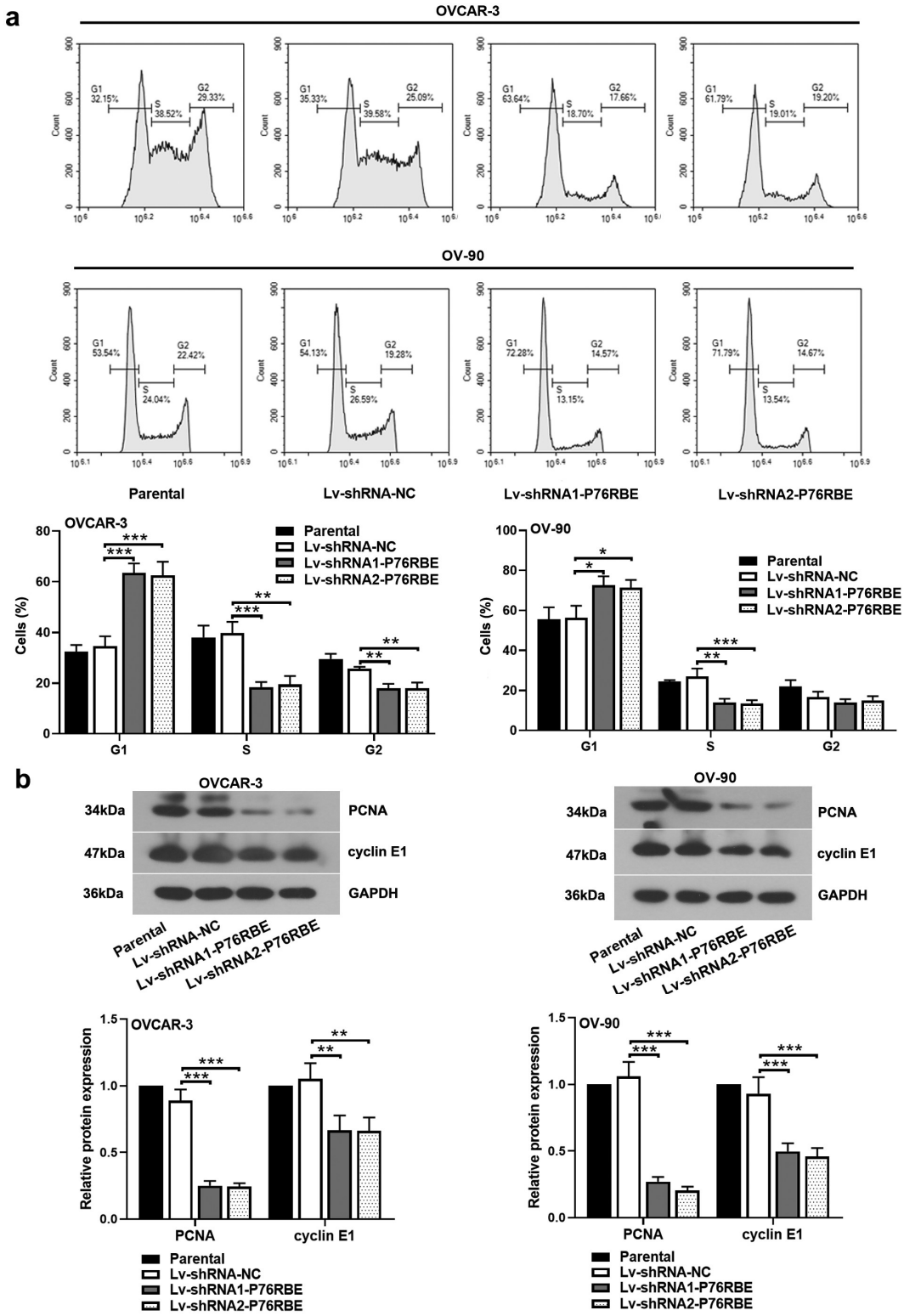

Figure 3. P76RBE knockdown arrests ovarian cancer cell cycle *in vitro*. (a) Cell cycle distribution was determined by flow cytometry in OVCAR-3 and OV-90 cells. The inhibition of P76RBE blocked ovarian cancer cells at G1 phase. (b) Western blot analysis was performed to ensure the cell cycle-related protein levels after P76RBE knockdown. * represents *vs*. Lv-shRNA-NC. *P < 0.05, **P < 0.01, ***P < 0.001.

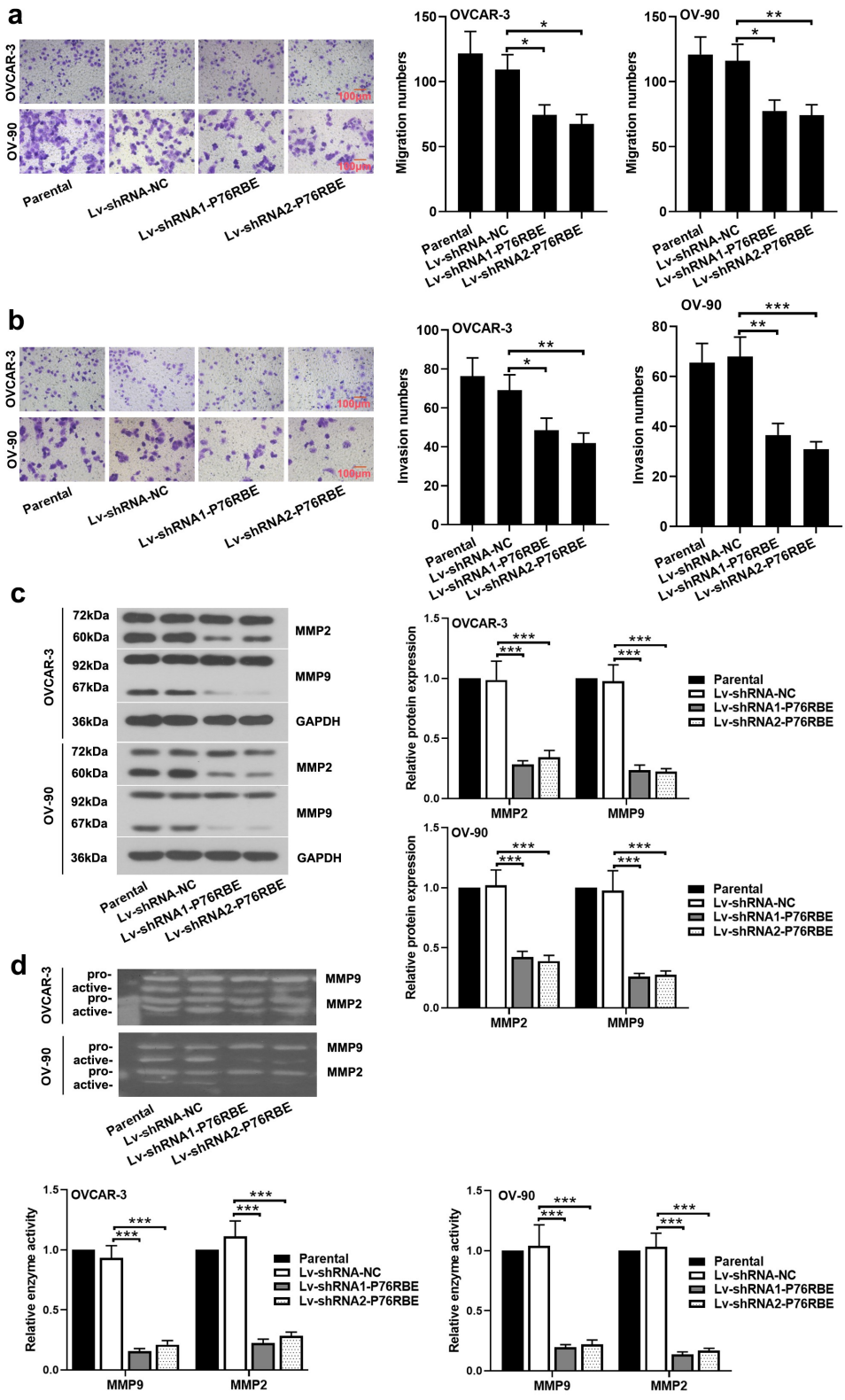

Figure 4. Silencing of P76RBE attenuates ovarian cancer cell migration and invasion *in vitro*. (a, b) The transwell chambers with or without Matrigel were executed to estimate the effect of P76RBE knockdown on cell invasion and migration both in OVCAR-3 and OV-90 cells. (scale bar = 100 μm). (c) The protein expression of MMP2 and MMP9 was monitored in P76RBE-silencing ovarian cancer cells. (d) In addition, the effect of P76RBE on MMP2 and MMP9 activities was determined via gelatin zymography. * represents *vs*. Lv-shRNA-NC. *P < 0.05, **P < 0.01, ***P < 0.001.

P76RBE knockdown on cell invasion and migration. The results implied that mobile (Figure 4(a)) and invasive (Figure 4(b)) abilities of cells were observably impaired when OVCAR-3 and OV-90 cells were stable infected lentiviral expressing P76RBE shRNA. In addition, the expression levels and activities of MMP2 and MMP9, two major matrix metalloproteinases that are able to accelerate the degradation of extracellular matrix, thereby increasing tumor cell invasion and migration, were also measured (Figure 4(c,d)). The data illustrated that the low expression of P76RBE repressed the protein levels and activities of MMP2 and MMP9. These findings indicated that P76RBE facilitated cell migration and invasion in ovarian cancer.

3.4. P76RBE silencing inhibits the activation of integrin β1/NF-κB pathway

To probe the mechanism by which P76RBE drives, the integrin β1/NF-κB pathway-associated factors were detected. Western blot analysis explained that P76RBEsilencing downregulated the expression of integrin β1 and suppressed the activation of NF-κB pathway. As shown in Figure 5(a,b), knocking down P76RBE inhibited the degradation of IκBα, phosphorylation of P65, and expression of COX2. To further validate our data, the immunofluorescence assay was performed to intuitively detect the translocation of P65. It was also found that P76RBE silencing inhibited the translocation of P65 to nucleus, thereby preventing NF-κB pathway activation (Figure 5(c)). Taken together, integrin β1 was a downstream factor of P76RBE and P76RBE regulated NF-κB pathway activation.

3.5. The aggravating effect of P76RBE-overexpressing on cell proliferation, migration, and invasion is reversed via repressing integrin β1 in vitro

A series of rescue experiments were performed to completely evidence the above argument. Here, P76RBE-overexpressing plasmid and integrin β1-silencing plasmid were transfected into A2780 cells, respectively. Transfection efficiency was confirmed by western blot (Figure 6(a,b)). Subsequently, MTT assay demonstrated that the elevated P76RBE promoted ovarian cancer cell viability, whilst the decreased integrin β1 reversed the increase of cell viability (Figure 6(c), $p < 0.05$). In addition, the results of transwell assays demonstrated that integrin β1 knockdown effectively rescued the effects of P76RBE overexpression on ovarian cancer cells with suppressed migration and invasion (Figure 6(d)). Meanwhile, we found that the levels of PCNA, MMP2, and MMP9 were significantly enhanced in cells transfected with overexpressed P76RBE, while integrin β1 silencing suppressed cell growth and metastasis (Figure 6(e)). Moreover, the data clarified that integrin β1 knockdown markedly attenuated P76RBE-stimulated the phosphorylation of P65 (Figure 6(f)). The results indicated that integrin β1 participated in P76RBE-mediated oncogenic behaviors in ovarian cancer.

3.6. P76RBE silencing restrains the tumor growth in vivo

The *in vivo* experiments were conducted in nude mice via injecting stable P76RBE knockdown cells (OVCAR-3 and OV-90). We observed that the tumor volumes in the two P76RBE knockdown groups were significantly smaller than those in the Lv-shRNA-NC group (Figure 7(a,b)). Additionally, the immunohistochemical analysis of P76RBE and integrin β1 reflected that P76RBE silencing diminished the expression of both P76RBE and integrin β1 in tumor tissues of nude mice (Figure 7(c,d)). Similarly, the protein levels of representative factors (PCNA, MMP2, P65, and p-P65) were assessed to further ascertain the effect of P76RBE (Figure 7(e,f)). As expected, P76RBE knockdown decreased the expression levels of PCNA, MMP2, and p-P65.

4. Discussion

Ovarian cancer affects millions of individuals worldwide, and we still need to continuously explore its pathogenesis for providing more opportunities. In this study, we observed the higher expression of P76RBE in ovarian cancer tissues and cells. Our data indicated that silencing of P76RBE obviously suppressed proliferation, migration, and invasion of ovarian cancer cells *in vitro* and *in vivo*. The aggravating effect of

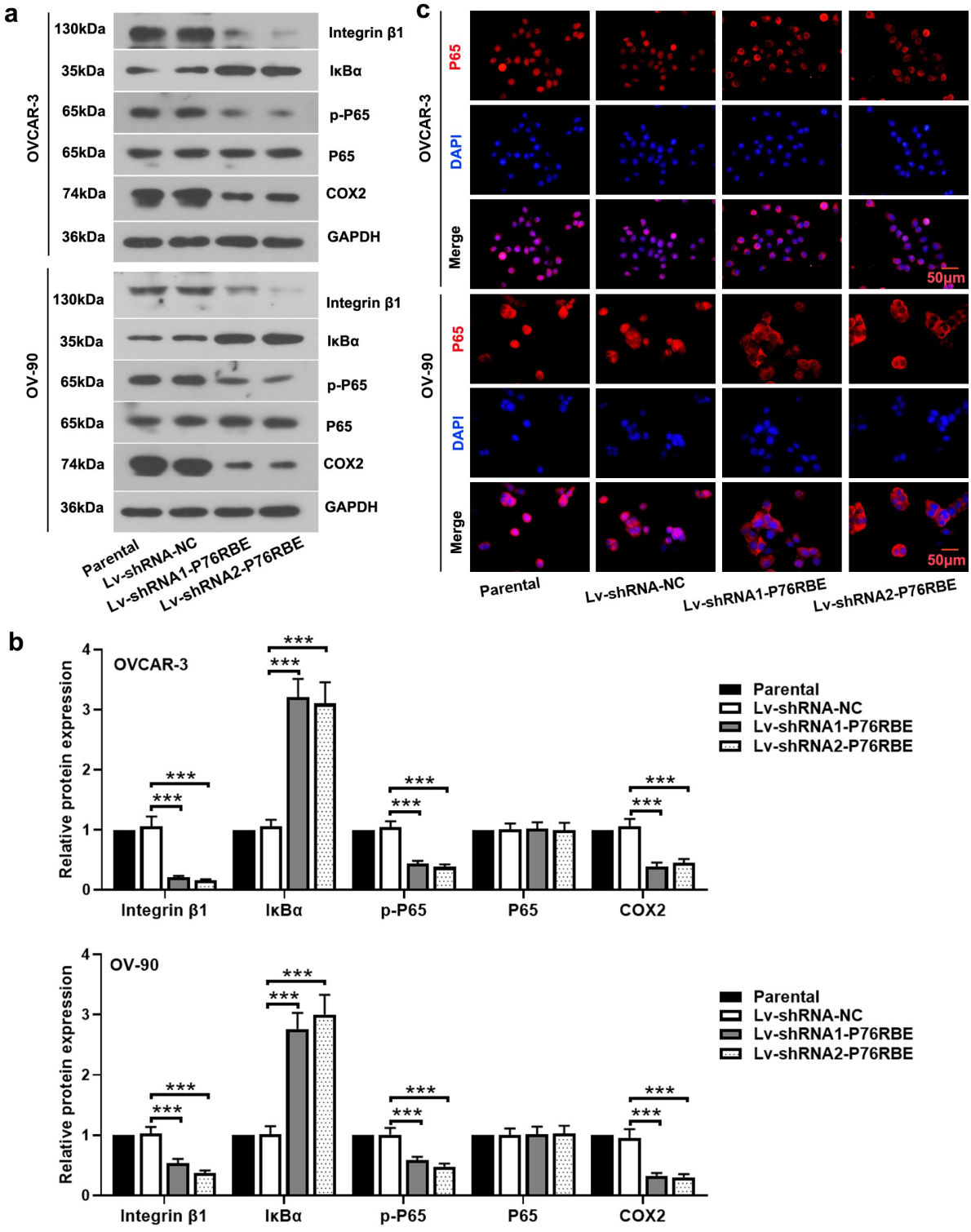

Figure 5. Inhibition of P76RBE alleviates the activation of integrin β1/NF-κB pathway. (a, b) Western blot analysis in P76RBE knockdown cell lines (OVCAR-3 and OV-90). The low expression of P76RBE decreased integrin β1 level, increased IκBα level, whilst decreased phosphorylation of P65 and COX2 expression. (c) Immunofluorescence assay showed the P65 expression and position. (scale bar = 50 μm).

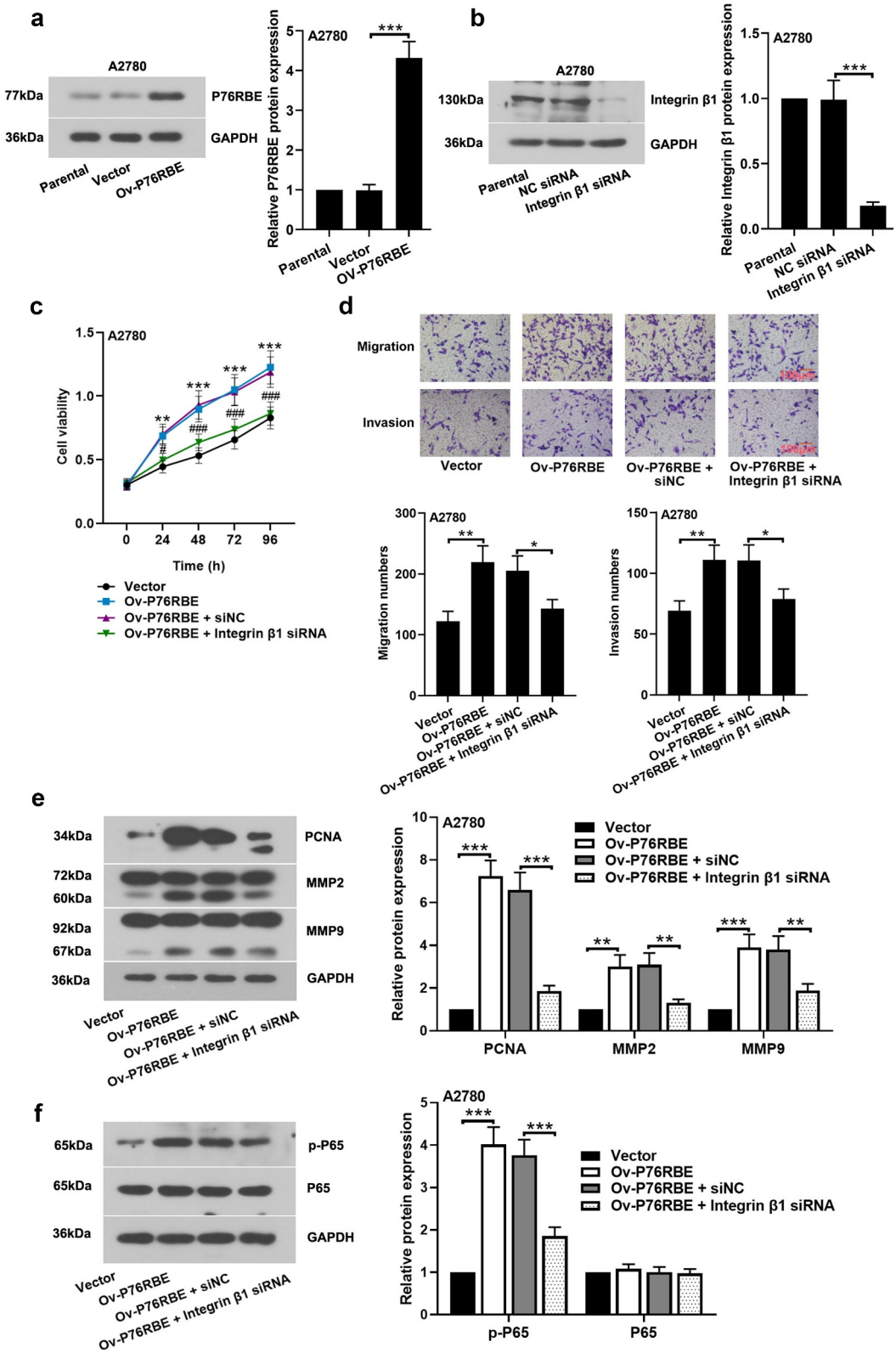

Figure 6. The aggravating effect of P76RBE-overexpressing on cell proliferation, migration and invasion is reversed via repressing integrin β1 *in vitro*. (a) The P76RBE expression was measured in A2780 cells transfected with P76RBE overexpression vector. (b) The integrin β1 expression was examined in integrin β1-silencing A2780 cells. (c) MTT assay was performed to confirm the cell viability after integrin β1 knockdown in P76RBE-overexpressing A2780 cells. (d) Migration and invasion ability of A2780 cells co-transfected with Ov-P76RBE and integrin β1 siRNA were detected by transwell assay (scale bar = 100 μm). (e) Cell proliferation and invasion-related proteins (PCNA, MMP2 and MMP9) were determined via western blot. (f) The representative factors of NF-κB pathway, P65 and p-P65, were analyzed using western blot. * represents *vs*. Vector. # represents *vs*. Ov-P76RBE + siNC. *P < 0.05, **P < 0.01, ***P < 0.001. #P < 0.05, ###P < 0.001.

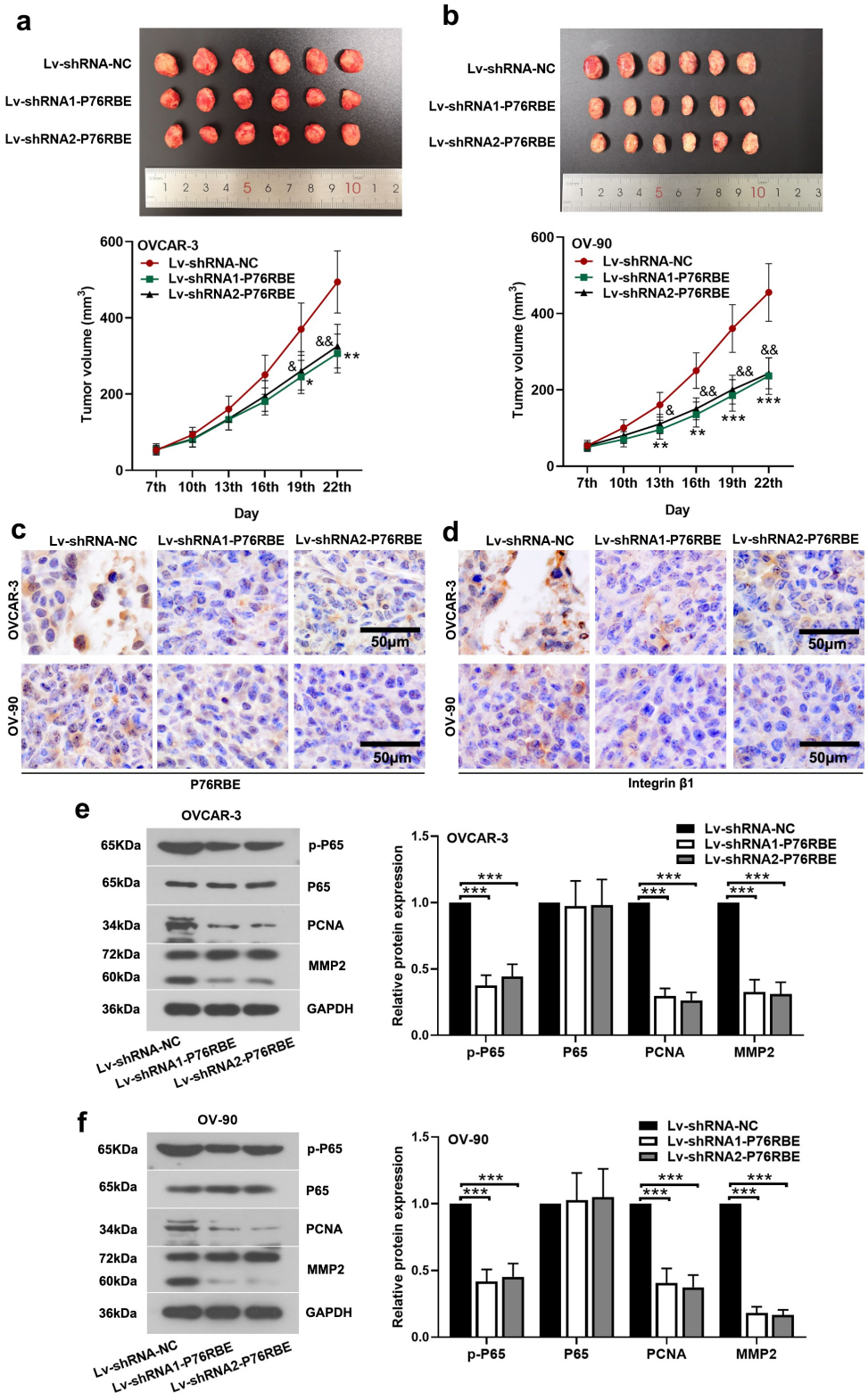

Figure 7. P76RBE silencing restrains the tumor growth *in vivo*. The nude mice were subcutaneously injected with cells (OVCAR-3 and OV-90) infected with Lv-shRNA-NC, Lv-shRNA1-P76RBE, and Lv-shRNA2-P76RBE, respectively. (a, b) The tumor volume was measured every 3 days. The images of tumor tissues were captured. The expression of P76RBE (c) and integrin β1 (d) was obtained via immunohistochemistry after P76RBE inhibition in nude mice (scale bar = 50 μm). (e, f) The protein levels of related factors (MMP2, PCNA, P65, and p-P65) were tested via western blot analysis in tumor tissues. * represents Lv-shRNA1-P76RBE *vs*. Lv-shRNA-NC. & represents Lv-shRNA2-P76RBE *vs*. Lv-shRNA-NC. *P < 0.05, **P < 0.01, ***P < 0.001. &P < 0.05, &&P < 0.01.

P76RBE-overexpressing on malignant behaviors was reversed through inhibiting integrin β1. Mechanistically, P76RBE promoted malignant phenotypes, which were regulated via activating integrin β1/NF-κB signaling in ovarian cancer cells.

The results from oncomine database and *in vitro* experiments demonstrated that P76RBE was upregulated, which implied a deteriorating effect on the progression of ovarian cancer. In the previous studies, P76RBE was increased in various cancers. For instance, the higher level of P76RBE was discovered in NSCLC tissues compared with adjacent normal tissues [7]. Danussi *et al.* researched that upregulated P76RBE derived mesenchymal transformation in malignant glioma [6]. In addition, our data still illustrated that the inhibition of P76RBE decreased ovarian cancer cell viability, arrested cell at G1 phase, and reduced proliferation-related factor levels (PCNA and cyclin E1). The similar results were observed in other groups. Huang *et al.* revealed that overexpression of miR-200a accelerated NSCLC cell apoptosis and repressed cell proliferation through downregulating P76RBE [7]. Jiang *et al.* also demonstrated that the suppression of P76RBE blocked cell proliferation of prostate cancer [5]. However, Danussi *et al.* found that P76RBE expression did not affect cell proliferation in malignant glioma. We speculated these different results may be due to different types of cancer.

Integrins are cell surface adhesion proteins binding with abundant category of extracellular ligands [19]. The enhancement of integrins is related to malignancy. There is growing evidence that integrin β1 is overexpressed in ovarian cancer cells and facilitated migration and invasion [13,14]. For example, in head and neck cancer, blocking the integrin β1 inhibited the cell metastatic ability [20]. Additionally, in gastric cancer, increasing integrin β1 stimulated lymph node metastasis [21]. Zeng *et al.* illustrated that silencing SPP1 restrained integrin β1 alleviating cell proliferation, migration, and invasion [22]. These were consistent with our results. Furthermore, our study elucidated the relationship between P76RBE and integrin β1 for the first time. Our data showed that integrin β1 was a vital downstream factor of P76RBE and participated in P76RBE-mediated oncogenic behaviors in ovarian cancer. As mentioned in our introduction, studies had confirmed that P76RBE was able to activate RhoA inducing mesenchymal phenotype in malignant glioma, and activation of RhoA may modulate downstream phosphorylation of Akt [23]. At the same time, AKT can also regulate the activity of integrin β1 [24,25]. Therefore, it is not difficult for us to conclude that P76RBE is capable to regulate integrin β1.

To further investigate whether NF-κB pathway takes part in P76RBE-mediated oncogenic behaviors, NF-κB pathway-related factors were determined. Our data demonstrated that diminishment of P76RBE suppressed degradation of IκBα and ameliorated phosphorylation of P65. In the meantime, it was found that P76RBE silencing inhibited the translocation of P65 to nucleus, thereby preventing NF-κB pathway activation. Our team firstly shed light on the relationship between P76RBE and NF-κB signaling. Furthermore, integrin β1 knockdown markedly attenuated P76RBE-stimulated the phosphorylation of P65. Similarly, Zeng *et al.* showed that increased integrin β1 expression and NF-κB signaling activation in metastatic osteosarcoma tissues, which intensified tumorigenesis [26]. All data suggest that P76RBE accelerates cell proliferation, migration, and invasion via activating integrin β1/NF-κB pathway.

In summary, P76RBE contributes to the cell proliferation, migration, and invasion in ovarian cancer. Especially, P76RBE facilitates malignant behaviors of ovarian cancer cells through activating the integrin β1/NF-κB pathway. Our study provides a promising therapeutic target for the diagnosis and treatment of ovarian cancer.

Acknowledgments

This study was supported by Natural Science Foundation of Liaoning Province (2019-ZD-0785), Young Backbone Teachers Project of China Medical University (QGZD2018063), 345 Talent Project of Shengjing Hospital of China Medical University..

Disclosure statement

The authors declare that they have no competing interests.

Funding

This study was supported by Natural Science Foundation of Liaoning Province (2019-ZD-0785), Young Backbone Teachers Project of China Medical University (QGZD2018063), 345 Talent Project of Shengjing Hospital of China Medical University.

Author contributions

Limei Yan performed experiments and wrote the manuscript. Zeping He, Wei Li, and Ning Liu performed experiments and analyzed the data. Song Gao designed this study and polished the manuscript.

References

[1] Webb PM, Jordan SJ. Epidemiology of epithelial ovarian cancer. Best Pract Res Clin Obstet Gynaecol. 2017;41:3–14.
[2] Hızlı D, Boran N, Yılmaz S, et al. Best predictors of survival outcome after tertiary cytoreduction in patients with recurrent platinum-sensitive epithelial ovarian cancer. Eur J Obstet Gynecol Reprod Biol. 2012;163:71–75.
[3] Brinkhuis M, Izquierdo MA, Baak JP, et al. Expression of multidrug resistance-associated markers, their relation to quantitative pathologic tumour characteristics and prognosis in advanced ovarian cancer. Anal Cell Pathol. 2002;24:17–23.
[4] Peck JW, Oberst M, Bouker KB, et al. The RhoA-binding protein, rhophilin-2, regulates actin cytoskeleton organization. J Biol Chem. 2002;277:43924–43932.
[5] Jiang S, Mo C, Guo S, et al. Human bone marrow mesenchymal stem cells-derived microRNA-205-containing exosomes impede the progression of prostate cancer through suppression of RHPN2. J Exp Clin Cancer Res. 2019;38:495.
[6] Danussi C, Akavia UD, Niola F, et al. RHPN2 drives mesenchymal transformation in malignant glioma by triggering RhoA activation. Cancer Res. 2013;73:5140–5150.
[7] Huang Y, Bao T, Li Z, et al. Function of miR-200a in proliferation and apoptosis of non-small cell lung cancer cells. Oncol Lett. 2020;20:1256–1262.
[8] He D, Ma L, Feng R, et al. Analyzing large-scale samples highlights significant association between rs10411210 polymorphism and colorectal cancer. Biomed Pharmacother. 2015;74:164–168.
[9] Dopeso H, Rodrigues P, Bilic J, et al. Mechanisms of inactivation of the tumour suppressor gene RHOA in colorectal cancer. Br J Cancer. 2018;118:106–116.
[10] Wang P, Li W, Peng J, et al. Clinicopathological significance of RhoA expression in digestive tract cancer: a systematic review and meta-analysis. Clin Lab. 2016;62:1955–1964.
[11] Liu CM, Ma JQ, Xie WR, et al. Quercetin protects mouse liver against nickel-induced DNA methylation and inflammation associated with the Nrf2/HO-1 and p38/STAT1/NF-kappaB pathway. Food Chem Toxicol. 2015;82:19–26.
[12] Malik M, Segars J, Catherino WH. Integrin β1 regulates leiomyoma cytoskeletal integrity and growth. Matrix Biol. 2012;31:389–397.
[13] Lau MT, So WK, Leung PC. Integrin β1 mediates epithelial growth factor-induced invasion in human ovarian cancer cells. Cancer Lett. 2012;320:198–204.
[14] Zhang L, Zou W. Inhibition of integrin β1 decreases the malignancy of ovarian cancer cells and potentiates anticancer therapy via the FAK/STAT1 signaling pathway. Mol Med Rep. 2015;12:7869–7876.
[15] Yang Z, Zhou X, Liu Y, et al. Activation of integrin β1 mediates the increased malignant potential of ovarian cancer cells exerted by inflammatory cytokines. Anticancer Agents Med Chem. 2014;14:955–962.
[16] Hagenbuchner J, Ausserlechner MJ. Targeting transcription factors by small compounds–current strategies and future implications. Biochem Pharmacol. 2016;107:1–13.
[17] Yang W, Liu L, Li C, et al. TRIM52 plays an oncogenic role in ovarian cancer associated with NF-kB pathway. Cell Death Dis. 2018;9:908.
[18] Hu Y, Liu JP, Li XY, et al. Downregulation of tumor suppressor RACK1 by helicobacter pylori infection promotes gastric carcinogenesis through the integrin β-1/NF-κB signaling pathway. Cancer Lett. 2019;450:144–154.
[19] Carbonell WS, DeLay M, Jahangiri A, et al. β1 integrin targeting potentiates antiangiogenic therapy and inhibits the growth of bevacizumab-resistant glioblastoma. Cancer Res. 2013;73:3145–3154.
[20] Kim SA, Kwon SM, Kim JA, et al. 5′-Nitroindirubinoxime, an indirubin derivative, suppresses metastatic ability of human head and neck cancer cells through the inhibition of Integrin β1/FAK/Akt signaling. Cancer Lett. 2011;306:197–204.
[21] Wang Z, Wang Z, Li G, et al. CXCL1 from tumor-associated lymphatic endothelial cells drives gastric cancer cell into lymphatic system via activating integrin β1/FAK/AKT signaling. Cancer Lett. 2017;385:28–38.
[22] Zeng B, Zhou M, Wu H, et al. SPP1 promotes ovarian cancer progression via Integrin β1/FAK/AKT signaling pathway. Onco Targets Ther. 2018;11:1333–1343.

[23] Wegiel B, Gallo DJ, Raman KG, et al. Nitric oxide-dependent bone marrow progenitor mobilization by carbon monoxide enhances endothelial repair after vascular injury. Circulation. 2010;121:537–548.
[24] Leinhäuser I, Richter A, Lee M, et al. Oncogenic features of the bone morphogenic protein 7 (BMP7) in pheochromocytoma. Oncotarget. 2015;6:39111–39126.
[25] Zhang B, Gu F, She C, et al. Reduction of Akt2 inhibits migration and invasion of glioma cells. Int J Cancer. 2009;125:585–595.
[26] Li R, Shi Y, Zhao S, et al. NF-κB signaling and integrin-β1 inhibition attenuates osteosarcoma metastasis via increased cell apoptosis. Int J Biol Macromol. 2019;123:1035–1043.